Articles

Novel Poly(2,3-diphenyl-1,4-phenylenevinylene) Derivatives Containing Long Branched Alkoxy and Fluorenyl Substituents: Synthesis, Characterization, and Their Applications for Polymer Light-Emitting Diodes

Kuei-Bai Chen, Hsing-Chuan Li, Chien-Kai Chen, Sheng-Hsiung Yang, Bing R. Hsieh, and Chain-Shu Hsu*

Department of Applied Chemistry, National Chiao Tung University, 1001, Ta-Hsueh Rd., Hsinchu 30010, Taiwan, R.O.C.

ABSTRACT: Two series of poly(2,3-diphenyl-1,4-phenylenevinylene) (DP-PPV) derivatives containing long branched alkoxy chains or fluorenyl substituents were synthesized. The branched alkoxy groups were introduced to enhance the solubility for spin-coating processes. Bulky fluorenyl groups with two hexyl chains on the 9-position were introduced to increase steric hindrance and prevent close packing of the main chain. By controlling the feed ratio of different monomers during polymerization, DP-PPV derivatives with high molecular weights were obtained. All synthesized polymers possess high glass transitions temperatures and thermal stabilities. The maximum photoluminescent emissions of the thin films are located between 498 and 564 nm. Cyclic voltammetric analysis reveals that the band gaps of these light-emitting materials are in the range from 2.4 to 2.5 eV. A double-layer electroluminescent device with the configuration of ITO/PEDOT/polymer 2/Ca/Al exhibited a low turn-on voltage (4.0 V), a very high external quantum efficiency (3.39 cd/A), and a high brightness (16 910 cd/m^2).

Introduction

Since the first report on polymer light-emitting diodes (PLED),[1] a number of π-conjugated polymers have been intensively investigated in order to fabricate devices for industrial applications.[2–4] Among them, poly(1,4-phenylenevinylene) (PPV) has attracted a great deal of attention in recent years because of its unique structure and highly electroluminescent properties.[5] However, the requirement of the precursor route and intrinsic insolubility restrict further development of PPV. Many PPV derivatives have been synthesized to investigate their potential applications. For example, poly[2-methoxy-5-(2′-ethylhexoxy)-1,4-phenylenevinylene] (MEH-PPV) is an orange-red emissive polymer and soluble in common organic solvents; thin films of MEH-PPV can be obtained from a spin-coating process.[6] Cyano-substituted poly(2,5-dialkoxy-1,4-phenylenevinylene) (CN-PPV) is a red emissive polymer with high electron affinities.[7,8] Silyl-substituted PPV is a greenish emissive material with a tendency to be easily charged by electrons rather than holes.[9,10]

In 1997, Hsieh et al. proposed a synthetic route to poly(2,3-diphenyl-1,4-phenylenevinylene) (DP-PPV) which exhibits high photoluminescence (PL) efficiency in the solid state.[11] Different substituents were then introduced on the 5-position of the phenyl ring to improve its properties. For example, highly phenylated DP-PPV

was synthesized to further improve PL efficiency.[12] Long alkyl chains were incorporated to improve the solubility of the polymer.[13] Liquid crystalline moieties or imidazole groups were also incorporated to achieve additional optical properties.[14,15] By following this synthetic route, monomers containing diversified functional groups are easily synthesized, and therefore soluble DP-PPV derivatives with high molecular weights are also easily obtained. Despite the advantages mentioned above, low device performance using DP-PPVs as active layers was found and thus restricts their potential use for display applications. The reasons for low device performance come from two parts. For those DP-PPVs with long alkyl groups, the regularly hexagonal structures of the main chain form strong π–π interaction and reduce electroluminescence (EL) efficiency.[16] For those DP-PPVs with bulky substituents on the phenyl ring, the large steric hindrance inhibits the hopping process of carriers between adjacent polymers.[15] The removal of the third substituent on the phenyl ring may provide the solution to highly luminescent materials.

In this study two series of DP-PPVs derivatives were designed to improve luminescent properties. In the first series long branched alkoxy groups were introduced on pendent phenyl ring on the main chain to improve the solubility. In the second series a novel DP-PPV structure with fluorenyl substituent was proposed. The fluorene was incorporated as pendant group to increase the steric hindrance, and hence the prevention of close chain packing is predictable. The two alkyl chains on the C-9

* Corresponding author: Tel +886-3-5131523, Fax +886-3-5131523, e-mail cshsu@mail.nctu.edu.tw.

Scheme 1. Synthesis of Monomer M1
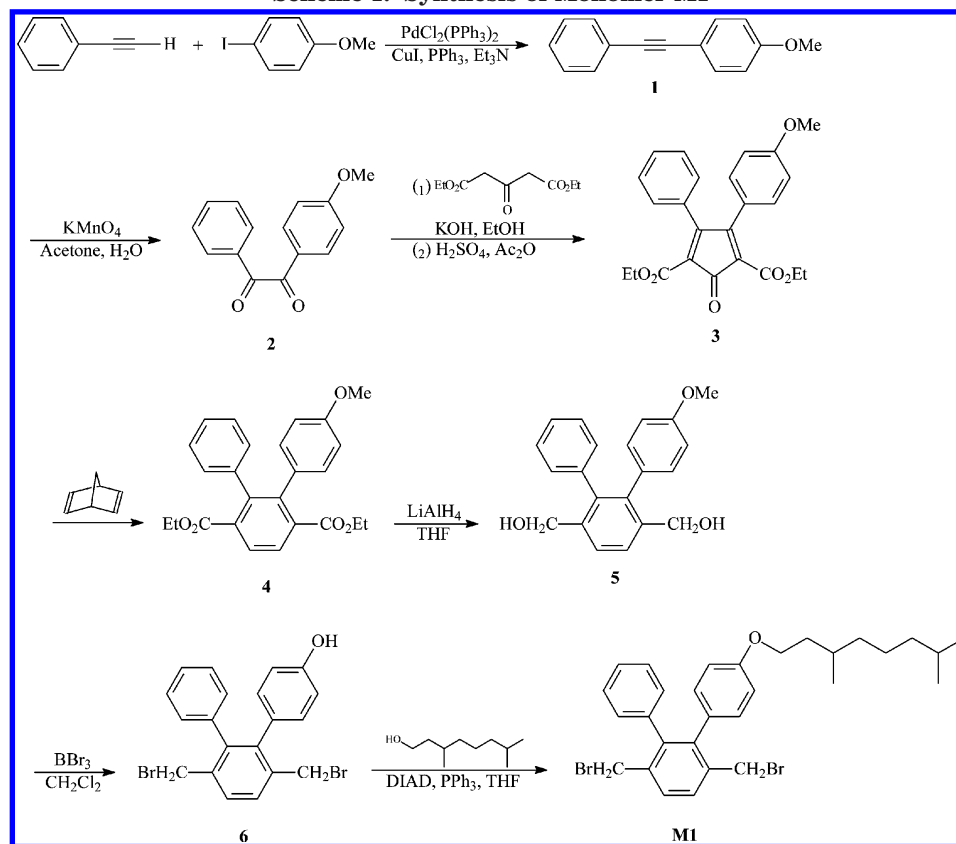
position may also help to increase the solubility. Five different DP-PPV precursors copolymerized with 2,5-dimethoxy- or 2-methoxy-5-(2′-ethylhexyloxy)-1,4-bis(bromomethyl)benzene were also made. The electrical and spectroscopic properties of theses polymers were systematically investigated. In addition, a series of PLED derives were also fabricated to study the electroluminescent (EL) properties of the polymers.

Experimental Section

Characterization Methods. ^{1}H NMR spectra were measured with a Varian 300 MHz spectrometer. Gel permeation chromatography (GPC) data assembled from a Viscotek T50A differential viscometer and a LR125 laser refractometer and three columns in series were used to measure the molecular weights of polymers relative to polystyrene standards at 35 °C. Differential scanning calorimetry (DSC) was performed on a Perkin-Elmer Pyris Diamond DSC instrument at a scan rate of 10 °C min^{-1}. Thermal gravimetric analysis (TGA) was undertaken on a Perkin-Elmer Pyris 1 TGA instrument with a heating rate of 10 °C min^{-1}. UV−vis absorption spectra were obtained with an HP 8453 diode array spectrophotometer. PL emission spectra were obtained using ARC SpectraPro-150 luminescence spectrometer. Cyclic voltammetric (CV) measurements were made in acetonitrile (CH$_3$CN) with 0.1 M tetrabutylammonium hexafluorophosphate (TBAPF$_6$) as the supporting electrolyte at a scan rate of 50 mV/s. Platinum wires were used as both the counter and working electrodes, silver/silver ions (Ag in 0.1 M AgNO$_3$ solution, from Bioanalytical Systems, Inc.) were used as the reference electrode, and ferrocene was used as an internal standard. The corresponding highest-occupied molecular orbital (HOMO) and lowest-unoccupied molecular orbital (LUMO) energy levels were estimated from the onset redox potentials.

Synthesis of Monomers M1−M4. All reagents and chemicals were purchased from commercial sources (Aldrich, Merck, Lancaster or TCI) and used without further purification. Tetrahydrofuran (THF) and dichloromethane (CH$_2$Cl$_2$) were

dried by distillation from sodium/benzophenone and calcium hydride, respectively. Schemes 1 and 2 list the synthetic routes for monomers **M1** and **M2**.

1-Methoxy-4-(2′-phenyl-1-ethynyl)benzene (1). To a solution of phenylacetylene (7.3 g, 71.7 mmol) in triethylamine (350 mL) was added 4-iodoanisole (16 g, 68.3 mmol), triphenylphosphine (PPh$_3$) (1.43 g, 5.46 mmol), CuI (0.54 g, 2.87 mmol), and PdCl$_2$(PPh$_3$)$_2$ (0.48 g, 0.683 mmol). The mixture was refluxed at 85 °C for 12 h. After cooling to room temperature, the crude product was filtered, washed with a large amount of *n*-hexane, and dried. It was purified by recrystallization from methanol to yield 12.1 g (85%) of white crystals; mp 54 °C. ^{1}H NMR (CDCl$_3$, δ, ppm): 3.81 (s, 3H, OC*H*$_3$), 6.86 (t, *J* = 8.4 Hz, 2H, aromatic-H), 7.29−7.32 (m, 3H, aromatic-H), 7.43−7.50 (m, 4H, aromatic-H).

4-Methoxybenzil (2). To a mixture of **1** (40 g, 0.192 mol), acetone (2000 mL), and distilled water (700 mL) KMnO$_4$ (152 g, 0.962 mol) was slowly added and stirred at room temperature for 4 h. After the reaction was completed, black MnO$_2$ solids were removed by filtration. The concentrated filtrate was extracted with 500 mL of ethyl acetate. The crude product was isolated by evaporating the solvent purified by recrystallization from methanol to yield 37.8 g (90%) of yellow crystals; mp 56 °C. ^{1}H NMR (CDCl$_3$, δ, ppm): 3.85 (s, 3H, −OC*H*$_3$), 6.9−7.2 (m, 2H, aromatic-H), 7.46−7.51 (m, 2H, aromatic-H), 7.60−7.65 (m, 1H, aromatic-H), 7.65−7.8 (m, 4H, aromatic-H).

2,5-Dicarbethoxy-3-(4′-methoxyphenyl)-4-phenylcyclopentanone (3). A mixture of **2** (40 g, 0.167 mol) and diethyl 1,3-acetonedicarboxylate (33.67 g, 0.167 mol) in ethanol (300 mL) and a solution of KOH (11.2 g, 0.2 mol) in ethanol (70 mL) were stirred at room temperature for 24 h. The resultant yellow precipitate was filtered off and dried. H$_2$SO$_4$ was then added dropwise with stirring to a slurry of the yellow precipitate in acetic anhydride (100 mL) until the solution became dark red. After 30 min, 50 g of ice was added slowly to decompose excess acetic anhydride, and the mixture was extracted with a large amount of water and ethyl acetate. The organic phase was concentrated in vacuo to give 44 g (65%) of deep-red liquid. ^{1}H NMR (CDCl$_3$, δ, ppm): 1.13−0.250 (m, 6H,

Scheme 2. Synthesis of Monomer M2
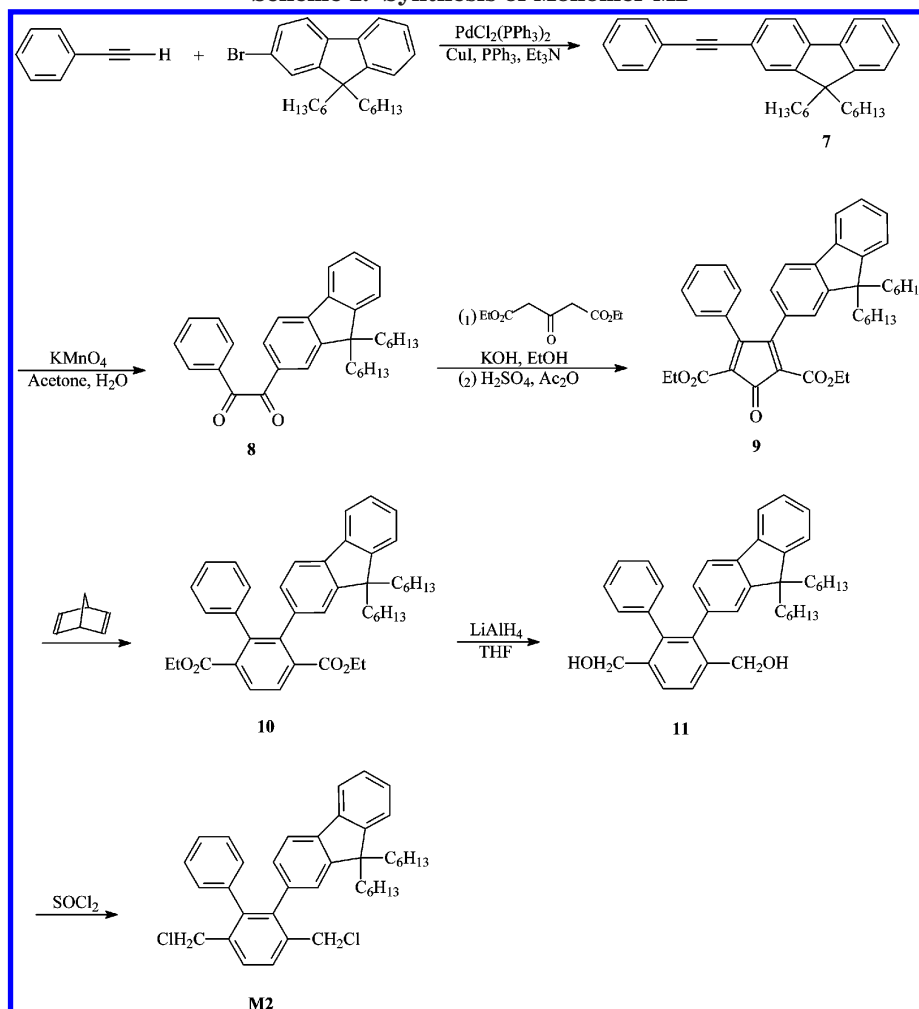
CO$_2$CH$_2$ C*H$_3$*), 3.8 (s, 3H, $-$OC*H$_3$*), 4.17$-$4.24 (m, 4H, CO$_2$C*H$_2$*-CH$_3$), 6.74 (d, *J* = 8.4 Hz, 2H, aromatic-H), 6.97 (m, 5H, aromatic-H), 7.26$-$7.42 (m, 3H, aromatic-H).

Diethyl-2-(4′-methoxyphenyl)-3-phenylterephalate (4). A mixture of **3** (35 g, 86.2 mmol) and norbornadiene (31.8 g, 0.345 mol) were dissolved in toluene (500 mL) and refluxed at 120 °C for 12 h. After cooling to room temperature, the solution was concentrated in vacuo to remove the solvent, and crude product was purified by recrystallization from methanol to give 25 g (70%) of white crystals; mp 95 °C. ¹H NMR (CDCl₃, *δ*, ppm): 0.83$-$0.96 (m, 6H,$-$CO$_2$CH$_2$C*H$_3$*), 3.72 (s, 3H, $-$OC*H$_3$*), 3.94$-$4.01 (m, 4H, $-$CO$_2$C*H$_2$*CH₃), 6.65 (t, *J* = 8.4 Hz, 2H, aromatic-H), 6.90 (t, *J* = 7.8 Hz, 2H, aromatic-H), 6.96 (m, 2H, aromatic-H), 7.02 (t, *J* = 7.2 Hz, 3H, aromatic-H), 7.73 (d, *J* = 8.0 Hz, 2H, aromatic-H).

1,4-Bis(hydroxymethyl)-2-(4′-methoxyphenyl)-3-phenylbenzene (5). A solution of **4** (10 g, 24.7 mmol) in THF (30 mL) was added dropwise with stirring to a suspension of LiAlH₄ (7.128 g, 0.198 mol) in THF (100 mL) at 0 °C under a nitrogen atmosphere. The solution was then refluxed at 70 °C for 4 h. After the solution was cooled in an ice bath, a saturated Na₂SO₄ aqueous solution was added dropwise until the solution became white. The white precipitate was removed by filtration. The crude product was isolated by evaporating the solvent purified by recrystallization from methanol to yield 7.8 g (98%) of white solid; mp 139 °C. ¹H NMR (CDCl₃, *δ*, ppm): 3.72 (s, 3H, OC*H$_3$*), 4.44 (s, 4H, C*H$_2$*OH), 6.82 (t, *J* = 8.4 Hz, 2H, aromatic-H), 6.90 (t, *J* = 7.8 Hz, 2H, aromatic-H), 6.96 (m, 2H, aromatic-H), 7.01 (t, *J* = 7.2 Hz, 3H, aromatic-H), 7.57 (s, 2H, aromatic-H).

1,4-Bis(bromomethyl)-2-phenoxy-3-phenylbenzene (6). To a solution of **5** (8.0 g, 25 mmol) in CH₂Cl₂ (50 mL) was slowly added 1.0 M boron tribromide (BBr₃) (113 mL, 0.113

mol) at 0 °C and was slowly added to a solution of **5** (8.08 g, 25 mmol) in CH₂Cl₂ (50 mL) under a nitrogen atmosphere. The solution was stirred at room temperature overnight. Water was then added dropwise into the solution to destroy unreacted BBr₃. The mixture was extracted with 10% NaHCO₃(aq), and the organic phase was concentrated in vacuo. The crude product was purified by gel chromatography (silica gel, hexane: ethyl acetate = 10:1 as the eluent) and recrystallized from *n*-hexane to give 6.8 g (63%) of white crystals; mp 128 °C. ¹H NMR (CDCl₃, *δ*, ppm): 4.24 (s, 2H, C*H$_2$*Br), 6.58 (m, 2H, aromatic-H), 6.87 (d, *J* = 8.4 Hz, 2H, aromatic-H), 6.99$-$7.03 (m, 2H, aromatic-H), 7.11$-$7.16 (m, 3H, aromatic-H), 7.51 (s, 2H, aromatic-H).

1,4-Bis(bromomethyl)-2-[4′-(3,7-dimethyloctoxy)phenyl]-3-phenylbenzene (M1). A mixture of **6** (3.0 g, 6.9 mmol), 3,7-dimethyloctanol (1.46 g, 9.0 mmol), and PPh₃ (2.42 g, 9. 0 mmol) were dissolved in anhydrous CH₂Cl₂ (50 mL), and a solution of diethyl azodicarboxylate (1.55 g, 9.0 mmol) in anhydrous CH₂Cl₂ (10 mL) at $-$20 °C was added slowly under a nitrogen atmosphere. The solution was stirred at room temperature overnight. The mixture was then washed with water and dried with anhydrous MgSO₄. The crude product was isolated by evaporating the solvent and further purified by gel chromatography (silica gel, hexane:ethyl acetate = 20:1 as the eluent) to give 1.56 g (39%) of white crystals; mp 44 °C. ¹H NMR (CDCl₃, *δ*, ppm): 0.83 (q, 9H, $-$OCH₂CH₂CH-(C*H$_3$*)(CH₂)₃CH(C*H$_3$*)₂), 1.10$-$1.30 (m, 8H, $-$OCH₂C*H$_2$*CH-(CH₃)(C*H$_2$*)₃CH(CH₃)₂), 1.75$-$1.85 (m, 2H, $-$OCH₂C*H$_2$*CH-(CH₃)(CH₂)₃CH(CH₃)₂), 3.86 (s, 2H, $-$OC*H$_2$*$-$), 4.24 (s, 2H, $-$C*H$_2$*Br), 6.646$-$6.673 (d, *J* = 8.4 Hz, 2H, aromatic-H), 6.9 (d, *J* = 7.8 Hz, 2H, aromatic-H), 7.01 (m, 2H, aromatic-H), 7.17 (t, *J* = 7.2 Hz, 3H, aromatic-H), 7.51 (s, 2H, aromatic-H).

9,9-Dihexyl-2-(2′-phenyl-1-ethynyl)fluorene (7). By following the procedure of **1** and using 2-bromo-9,9-dihexylfluorene as starting material, the compound **7** was obtained as white crystals with mp 67 °C (85% yield). ^{1}H NMR (CDCl$_3$, δ, ppm): 0.85−1.01 (t, J = 6.8 Hz, 6H, fluorene-(CH$_2$)$_4$-CH$_2$CH_3), 1.23−1.44 (m, 16H, fluorene-CH$_2$-(CH_2)$_4$-CH$_3$), 2.56−2.84 (m, 4H, fluorene-CH_2-(CH$_2$)$_4$-CH$_3$), 6.99−7.08 (m, 2H, aromatic-H), 7.16−7.27 (m, 7H, aromatic-H), 7.44−7.47 (m, 12H, aromatic-H), 7.59−7.61 (m, 1H, aromatic-H).

1-(9,9-Dihexyl-2-fluorenyl)-2-phenyl-1,2-ethanedione (8). By following the procedure of **2** and using **7** as starting material, compound **8** was obtained as a deep-yellow liquid (93% yield). ^{1}H NMR (CDCl$_3$, δ, ppm): 0.91−0.94 (t, J = 6.8 Hz, 6H, fluorene-(CH$_2$)$_4$-CH$_2$CH_3), 1.23−1.44 (m, 16H, fluorene-CH$_2$-(CH_2)$_4$-CH$_3$), 2.56−2.84 (m, 4H, fluorene-CH_2-(CH$_2$)$_4$-CH$_3$), 6.99−7.03 (m, 1H, aromatic-H), 7.25−7.29 (m, 1H, aromatic-H), 7.43−7.45 (d, J = 7.0 Hz, 1H, aromatic-H), 7.48−7.59 (m, 3H, aromatic-H), 7.70−7.74 (m, 4H, aromatic-H), 7.80 (s, 1H, aromatic-H).

Diethyl 4-(9,9-Dihexyl-2-fluorenyl)-2-oxo-5-phenyl-3,5-cyclopentadiene-1,3-dicarboxylate (9). By following the procedure of **3** and using **8** as starting material, compound **9** was obtained as deep-red liquid (74% yield). ^{1}H NMR (CDCl$_3$, δ, ppm): 0.87−0.93 (t, J = 6.8 Hz, 6H, fluorene-(CH$_2$)$_4$-CH$_2$CH_3), 1.23−1.44 (m, 16H, fluorene-CH$_2$-(CH_2)$_4$-CH$_3$), 1.44−1.48 (m, 6H, CO$_2$CH$_2$CH$_3$), 2.56−2.84 (m, 4H, fluorene-CH_2-(CH$_2$)$_4$-CH$_3$), 4.31−4.36 (m, 4H, CO$_2$CH_2CH$_3$), 6.82 (d, J = 7.0 Hz, 1H, aromatic-H), 6.99−7.09 (m, 2H, aromatic-H), 7.24−7.31 (m, 2H, aromatic-H), 7.38−7.53 (m, 4H, aromatic-H), 7.61−7.66 (m, 2H, aromatic-H), 7.92 (s, 1H, aromatic-H).

Diethy 2-Phenyl-3-(9,9-dihexylfluoren-2-yl)terephthalate (10). By following the procedure of **4** and using **9** as starting material, compound **10** was obtained as a brown oil (75% yield). ^{1}H NMR (CDCl$_3$, δ, ppm): 0.91−0.94 (t, J = 6.8 Hz, 6H, fluorene-(CH$_2$)$_4$-CH$_2$CH_3), 1.28−1.32 (t, 6H, −CO$_2$CH$_2$CH_3), 1.23−1.44 (m, 16H, fluorene-CH$_2$-(CH_2)$_4$-CH$_3$), 1.44−1.48 (m, 6H, −CO$_2$CH$_2$CH_3), 2.56−2.84 (m, 4H, fluorene-CH_2-(CH$_2$)$_4$-CH$_3$), 4.21−4.27 (m, 4H, −CO$_2$CH_2CH$_3$), 6.52 (d, J = 7.0 Hz, 1H, aromatic-H), 6.99−7.05 (m, 2H, aromatic-H), 7.17−7.39 (m, 7H, aromatic-H), 7.59−7.60 (d, J = 7.6 Hz, 1H, aromatic-H), 7.74−7.76 (s, 1H, aromatic-H), 8.01−8.08 (m, 2H, aromatic-H).

1,4-Bis(hydroxymethyl)-2-phenyl-3-(9,9-dihexylfluoren-2-yl)benzene (11). By following the procedure of **5** and using **10** as starting material, compound **11** was obtained as yellow crystals with mp 185 °C (90% yield). ^{1}H NMR (CDCl$_3$, δ, ppm): 0.91−0.94 (t, 6H, fluorene-(CH$_2$)$_4$-CH$_2$CH_3), 1.23−1.44 (m, 16H, fluorene-CH$_2$-(CH_2)$_4$-CH$_3$), 2.56−2.84 (m, 4H, fluorene-CH_2-(CH$_2$)$_4$-CH$_3$), 4.90 (m, 4H, −CH_2OH), 6.99−7.40 (m, 10H, aromatic-H), 7.46−7.48 (d, J = 7.6 Hz, 1H, aromatic-H), 7.59−7.60 (m, 1H, aromatic-H), 7.75−7.77 (s, 1H, aromatic-H).

1,4-Bis(chloromethyl)-2-phenyl-3-(9,9-dihexylfluoren-2-yl)benzene (M2). To a solution of **11** (1.0 g, 1.83 mmol) in anhydrous CH$_2$Cl$_2$ (10 mL), 5 mL of thionyl chloride (SOCl$_2$) was added and stirred overnight under a nitrogen atmosphere. Water was then added dropwise into the solution to destroy excess thionyl cloride. The mixture was extracted with 10% NaHCO$_3$(aq), and the organic phase was concentrated in vacuo. The crude product was purified by gel chromatography (silica gel, hexane:ethyl acetate = 10:1 as the eluent) to give a pale-yellow liquid (1.1 g, 94%). ^{1}H NMR (CDCl$_3$, δ, ppm): 0.91−0.94 (t, J = 6.8 Hz, 6H, fluorene-(CH$_2$)$_4$-CH$_2$CH_3), 1.23−1.44 (m, 16H, fluorene-CH$_2$-(CH_2)$_4$-CH$_3$), 2.56−2.84 (m, 4H, fluorene-CH_2-(CH$_2$)$_4$-CH$_3$), 5.02 (m, 4H, −CH_2Cl), 6.99−7.40 (m, 10H, aromatic-H), 7.46−7.48 (d, J = 7.6 Hz, 1H, aromatic-H), 7.59−7.60 (m, 1H, aromatic-H), 7.75−7.77 (s, 1H, aromatic-H).

1,4-Bis(bromomethyl)-2,5-dimethoxybenzene (M3) and 1,4-Bis(bromomethyl)-2-methoxy-5-(2′-ethylhexoxy)benzene (M4). Monomers **M3** and **M4** were synthesized as described previously in the literature.[17,18]

Synthesis of Polymers: General Procedure. Scheme 3 outlines the synthesis of polymers **P1**−**P7**. An experimental procedure for the polymer **P1** is given below. To a solution of

Scheme 3. Synthesis of Polymers P1−P7
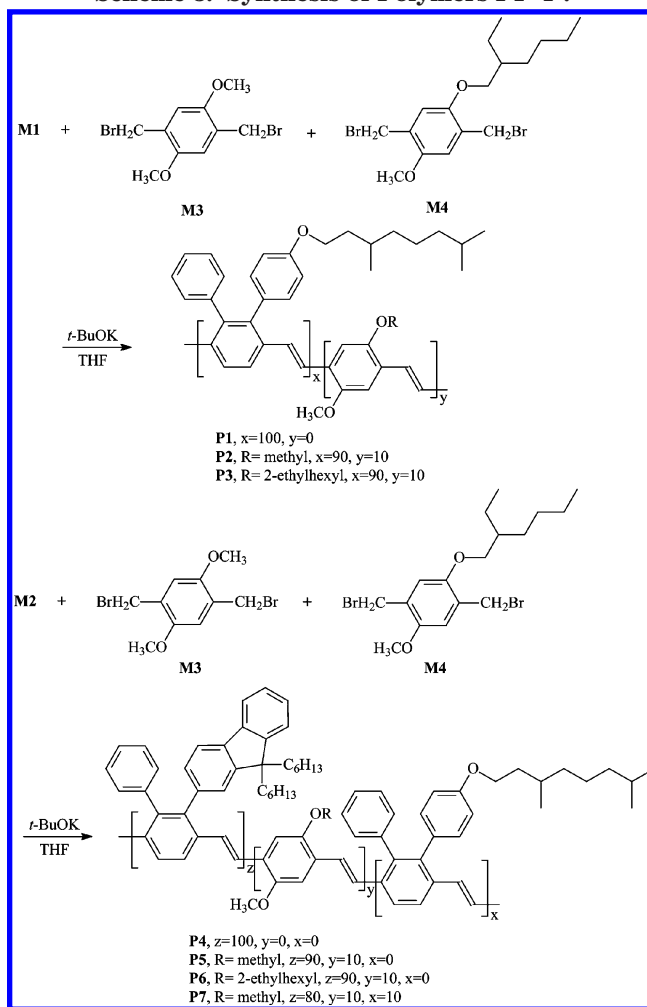
the monomer **M1** (1.43 g, 2.5 × 10^{-3} M) in THF (100 mL), a solution of potassium *tert*-butoxide (*tert*-BuOK, 12 equiv) in THF (20 mL) was added. The resulting mixture was stirred at room temperature for 24 h under a nitrogen atmosphere. A solution of 2,6-di-*tert*-butylphenol (6 equiv) as end-capping agent in THF (20 mL) was then added and stirred for 6 h. The polymer was obtained by pouring the mixture into methanol and filtered. It was purified by dissolving in THF and reprecipitated from methanol twice. After drying under vacuum for 24 h, the polymer was obtained as a yellow solid (0.53 g, 52%).

Device Fabrication and Measurements. Double-layer devices were fabricated as sandwich structures between calcium (Ca) cathodes and indium−tin oxide (ITO) anodes. ITO-coated glass substrates were cleaned sequentially in ultrasonic baths of detergent, 2-propanol/deionized water (1:1 volume) mixture, toluene, deionized water, and acetone. A 50 nm thick hole injection layer of poly(ethylenedioxythiophene) (PEDOT) doped with poly(styrenesulfonate) (PSS) was spin-coated on top of ITO from a 0.7 wt % dispersion in water and dried at 150 °C for 1 h in a vacuum. Thin films of synthesized polymers were spin-coated from toluene solutions onto the PEDOT layer and dried at 50 °C overnight in a vacuum. The thickness of the active layer was ca. 50 nm. Finally, 35 nm Ca and 100 nm Al electrodes were made through a shadow mask onto the polymer films by thermal evaporation using an AUTO 306 vacuum coater (BOC Edwards, Wilmington, MA). Evaporations were carried out typically at base pressures lower than 2 × 10^{-6} Torr. The active area of each EL device was 4 mm^2, and the device was characterized following a published protocol.[19]

Table 1. Feed Ratio and Polymerization Results of Polymers P1−P7

polymer	R	x	y	z	yield (%)	$\overline{M}_n$ $(\times 10^{-5})$	$\overline{M}_w$ $(\times 10^{-5})$	PDI
P1		100	0		52	2.78	4.27	1.54
P2	methyl	90	10		54	2.09	3.97	1.9
P3	2-ethylhexyl	90	10		54	2.89	4.78	1.65
P4		0	0	100	57	3.74	5.14	1.37
P5	methyl	0	10	90	55	2.66	3.97	1.49
P6	2-ethylhexyl	0	10	90	61	6.11	7.09	1.16
P7	methyl	10	10	80	51	3.9	4.55	1.14

Results and Discussion

Synthesis of Polymers. One standard approach to prepare soluble PPV derivatives is via the Gilch route using excess base to carry out the polymerization. The Gilch route employs α,α′-dihalo-*p*-xylene with *tert*-BuOK in organic solvents. Alkyl or alkoxy chains are often incorporated on the aromatic rings to improve the solubility of the resulting polymers. The polymerization condition is mild, and the molecular weights of obtained polymers are relatively large. However, there may be drawbacks. For example, gelation or precipitation of polymeric products may occur during polymerization. Ferraris et al. proposed a general synthetic method to carry out the Gilch route by reversed addition of base and using 4-methoxyphenol as an end-capping agent to prepare MEH-PPV.[18] For monomers **M1** and **M2** in this study, the pendent groups on the benzene ring, i.e., 2-[4′-(3,7-dimethyloctoxy)phenyl]-3-phenyl or 2-(9,9-dihexyl-fluorene)-3-phenyl, are quite bulky; this helps to minimize gelation and to improve the solubility of polymers. Even copolymerizing with monomers **M3** or **M4**, the resulting polymers are still soluble in common organic solvents, and no gelation was observed during polymerization.

Table 1 summarizes the feed ratio of monomers, molecular weights, and polydispersity index (PDI) of resulting polymers. The weight-average molecular weights ($\overline{M}_w$) of these polymers are in the range from 3.97×10^5 to 7.09×10^5, and PDI ($\overline{M}_w/\overline{M}_n$) is less than 2. The molecular weights of copolymers **P3** and **P6** are larger than those of their corresponding homopolymers **P1** and **P4**, while copolymers **P2** and **P5** showed smaller molecular weights. The benefit is seen that copolymerizing with **M4** increases the molecular weight, which resulted from the introduction of the branched 2-ethylhexoxy group. Copolymerizing with dimethoxy-substituted monomer **M3** restricted the growth of polymer chains and decreased the molecular weight. Nevertheless, the molecular weights of polymers **P1**−**P7** are very large, and the molecular weight distribution is relatively narrow. All obtained polymers can be dissolved in common organic solvents, such as chloroform, toluene, and chlorobenzene. Transparent and self-standing films can be cast from their solutions.

Thermal Properties. Table 2 summarizes the thermal properties of polymers **P1**−**P7**. Most polymers show good thermal stabilities with high glass temperature (T_g) over 140 °C and high decomposition temperatures (T_d) over 400 °C. Polymers **P4**−**P6** show even higher T_g than the others, which is attributed to the rigid fluorenyl group on the benzene ring. On the other hand, polymer **P7** shows lowest T_g and T_d which resulted from the random structure of three different repeating units. All synthesized materials possess good thermal properties which are important advantages in the fabrication of light-emitting devices.

Table 2. Thermal and Optical Properties of Polymers P1−P7

polymer	T_g (°C)	T_d (°C)	UV−vis (nm)		PL (nm)	
			solution	film	solution	film
P1	145	423	422	436	492	498
P2	145	439	439	441	520	545
P3	147	432	443	446	520	541
P4	178	417	442	444	481	498
P5	179	435	443	444	509	536
P6	171	434	449	454	519	526
P7	136	409	448	450	518	539

Optical Properties. Figure 1 shows the UV−vis absorption spectra of some synthesized materials in thin film state. Table 2 summarizes the UV−vis absorption maxima of all polymers in different states. The absorption maxima of synthesized polymers in toluene are located in the range from 422 to 449 nm which is attributed to the π−π* transition along the conjugated backbone. A red shift of the absorption band in thin film state is observed due to the effect of interchain π-stacking.[20] By comparing UV−vis absorption results of homopolymers and copolymers, copolymerizing with **M3** or **M4** results in red-shifted absorption because of the electron-donating alkoxy group. Furthermore, the fluorenyl substituent is rigid and bulky and results in a smaller red shift in copolymers **P5**−**P7**.
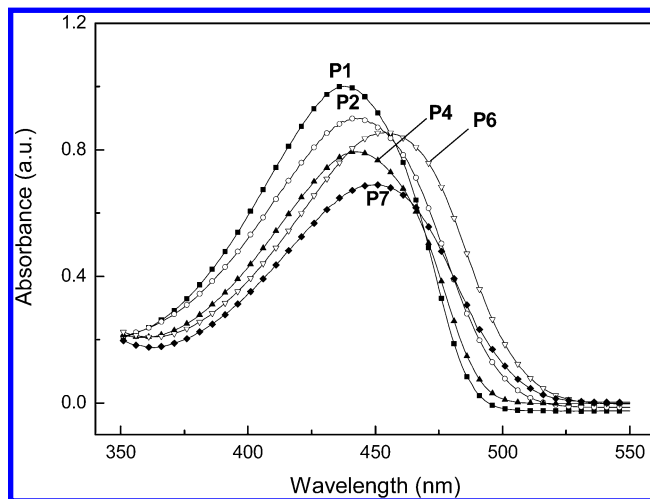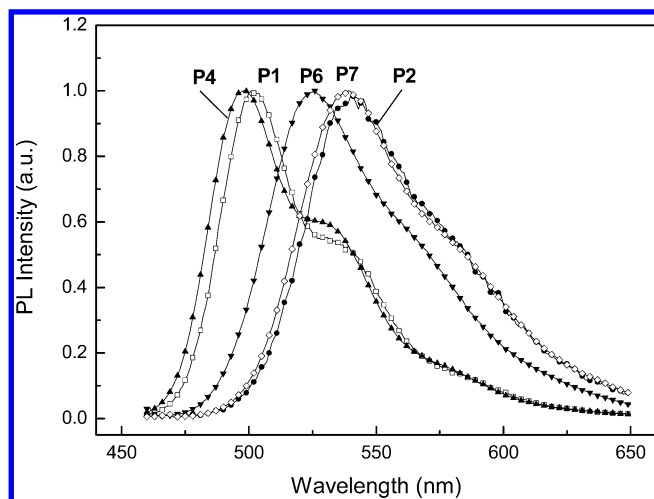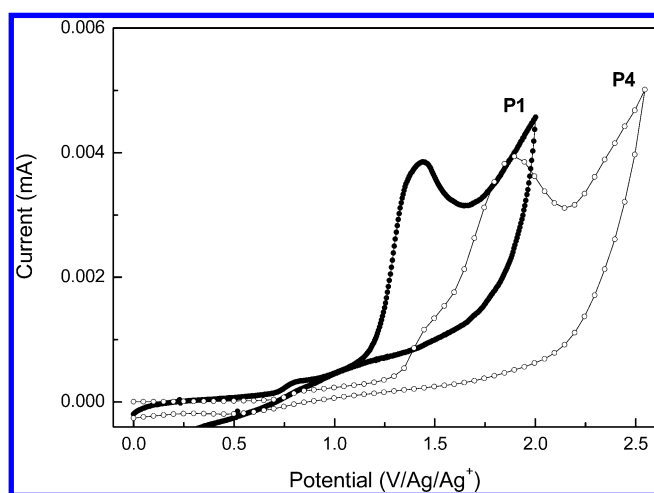

Figure 1. UV−vis absorption spectra of polymers **P1**, **P2**, **P4**, **P6**, and **P7** in thin film state.

Figure 2 reveals the PL emission spectra of some synthesized polymers in thin film state. The PL emission maxima in different states are also summarized in Table 2. The maximum emission bands are located from 481 to 520 nm in solution state and from 498 to 545 nm in thin film state. A similar tendency of the red shift from solution to thin film state is also observed. Homopolymers **P1** and **P4** show a clear emission shoulder band at 520 and 540 nm, respectively. How-

Figure 2. PL emission spectra of polymers **P1**, **P2**, **P4**, **P6**, and **P7** in thin film state.

Figure 3. Cyclic voltammograms of homopolymers **P1** and **P4**.

Table 3. Electrochemical Properties of Polymers P1–P7 in Solid Films

polymer	E_{ox} (V)	HOMO (eV)	UV edge (nm)	EG (eV)	LUMO (eV)
P1	1.2	−5.6	509	2.5	−3.1
P2	1.1	−5.5	523	2.4	−3.1
P3	1.2	−5.6	517	2.4	−3.2
P4	1.3	−5.7	493	2.5	−3.2
P5	1.2	−5.6	504	2.4	−3.2
P6	1.1	−5.5	503	2.5	−3.0
P7	1.2	−5.6	503	2.5	−3.1

which are in the range from 2.4 to 2.5 eV. Combining the electrochemical data and UV–vis characteristics gives an estimate of the LUMO energy levels. Table 3 summarizes the HOMO, LUMO, and EG values of polymers **P1**–**P7**. The energy level diagram of these materials is illustrated in Figure 4. Because of limited accuracy of CV measurement, the values of E_{ox}, HOMO, and LUMO are described to the first digit after the decimal point. Though the electrochemical values of these polymers are close, some tendencies can still be observed. For example, the relatively low oxidation potential (E_{ox}) of **P2** and **P6** reveals that they are favored for p-doping process compared with other polymers. The smaller energy barrier between polymer **P2** (or **P6**, **P7**) and PEDOT layer also shows the benefit for hole injection. Turning to EA value, all polymers have a quite small energy barrier of 0.1–0.3 eV to the cathode Ca. This implies that the synthesized polymers are favored for electron injection. Combining the electrochemical data obtained above, one can predict that polymers **P2**, **P6**, and **P7** may serve as good active layers in light-emitting devices.

Device Performance. Double-layer light-emitting diodes with the configuration of ITO/PEDOT/polymer/Ca/Al were fabricated to evaluate the potential of synthesized DP-PPV derivatives. The maximum EL emission bands of these polymers are listed in Table 4. The EL emissive maxima are located from 500 to 548 nm. The CIE coordinates of seven polymers are also shown in Table 3, referring to green (**P1**, **P4**, **P6**), green-yellow (**P2**, **P5**, **P7**), and yellow-orange light (**P3**). The EL emission spectra were similar to PL ones for polymers **P1**–**P4**. For polymers **P5**–**P7**, the maximum emission band shows significant differences of 6–11 nm between PL and EL spectra. The blue shift of the EL emission band increases as the operation voltage increases. The reason for the blue-shifted EL at high voltage is explained as follows. The structure of the polymer chain is normally obtained as head–tail type during the Gilch polymerization, as illustrated in Scheme 3. However, some head–head or tail–tail isomers may also form.[12] The head–head isomer owns the most strain energy due to bulky fluorenyl or long alkylphenyl group and is the least favorable. The tail–tail isomer has the least strain energy and, consequently, may be more favorable. Hence, several different conjugation lengths exist in these polymers. The head–head isomer has the shortest conjugation length or, in other words, has the largest band gap. At low voltage the head–tail and tail–tail blocks are activated to emit light, while head–head blocks are not. As the applied voltage increases, the head–head blocks are ultimately stimulated and the device emits a blue-shifted light. In this case the head–head block can be regarded as charge-trapping or defect site which owns a higher energy level.

Figure 5 shows the luminescence–voltage characteristics of some devices. The device using homopolymer

ever, the shoulder band of copolymers is not significant to observe. This may be due to random structures of polymer main chains which prevent close packing of neighboring polymers. A smaller full width in half-maximum (fwhm) is obtained and helps to improve color purity.

Electrochemical Analysis. Cyclic voltammetry (CV) was employed to investigate the electrochemical behaviors of synthesized polymers and to estimate their energy levels. The oxidation process is clear and directly associated with the conjugation structure of the polymer. However, the reduction process is usually irreversible and poorly defined. This behavior may associate with polymer defects or traces of impurities.[21] Figure 3 shows cyclic voltammograms of some polymers in the oxidation process. The HOMO energy level is determined from the onset of the oxidation curve (E_{ox}), which is given by

$$\text{HOMO (eV)} = -|E_{ox} + 4.4|$$

which are in the range from −5.7 to −5.4 eV. The energy gaps (EG) of materials are determined from the edge of their UV–vis absorption spectra (λ_{onset}), which is given by
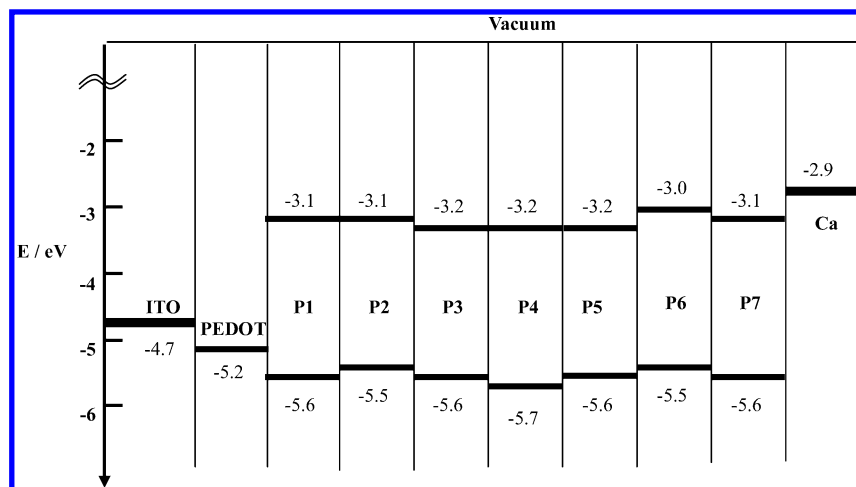
$$\text{EG (eV)} = 1240/\lambda_{onset}$$

Figure 4. Energy level diagrams of polymers **P1**−**P7**.

Table 4. Device Performance of Polymers P1−P7 in ITO/PEDOT/Polymer/Ca/Al Devices

polymer	EL (nm)	$V_{turn-on}$ (volt)	max brightness (cd/m^2)	max yield (cd/A)	CIE′ 1931	
					x	y
P1	504	6	303	0.69	0.27	0.59
P2	540	4	16910	3.39	0.39	0.58
P3	548	5	1936	6.14	0.43	0.56
P4	500	6	438	0.23	0.26	0.57
P5	528	5	1990	1.91	0.37	0.59
P6	520	4	6100	0.45	0.32	0.59
P7	528	3	14070	1.51	0.37	0.59

P1 as active layer showed an ordinary performance with a maximum brightness of 303 cd/m^2 at 10 V and a maximum current efficiency of 0.69 cd/A at 8 V. Using copolymer **P2** as active layer the device showed a tremendously improved brightness of 16 910 cd/m^2 at 10 V. The luminescence is highly improved by incorporating 2,5-dimethoxy-1,4-phenylenevinylene unit. The device of **P3** showed the best current efficiency of 6.14 cd/A at 8 V in the first series of DP-PPV derivatives. The device performance of these DP-PPV derivatives is summarized in Table 4.

In the second series of materials with fluorenyl substituent on the main chain, the device of homopolymer **P4** showed a maximum brightness of 438 cd/m^2 at 10 V and a maximum current efficiency of 0.23 cd/A at 8 V. By copolymerizing with **M3** or **M4** the device performance is further improved. A highly bright device using copolymer **P7** as an active layer was obtained with a maximum brightness of 14 070 cd/m^2 at 13 V and a maximum current yield of 1.51 cd/A at 5 V. The brightness and current density of these devices demonstrate significant enhancement as compared with previous reports.[12,15]

Mobility Measurement. The better performance of devices using **P2**, **P6**, or **P7** as active layer can be approximately explained by the smaller energy barrier among seven polymers. Generally speaking, a smaller barrier between PEDOT and polymer layer is helpful for hole injection. Smaller barrier between cathode and polymer layer is favored for electron injection. Polymers **P2**, **P6**, and **P7** are consistent with this situation, and more hole/electron can be injected into polymers and thus higher opportunity of recombination occurs here. In addition to the ease of charge injection, one important factor that affects the luminescence and current efficiency is the hole/electron mobility inside polymer layers. To further understand the exact reason for
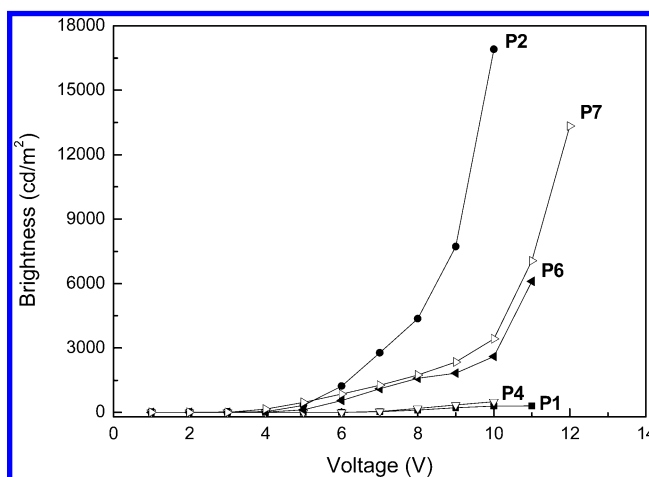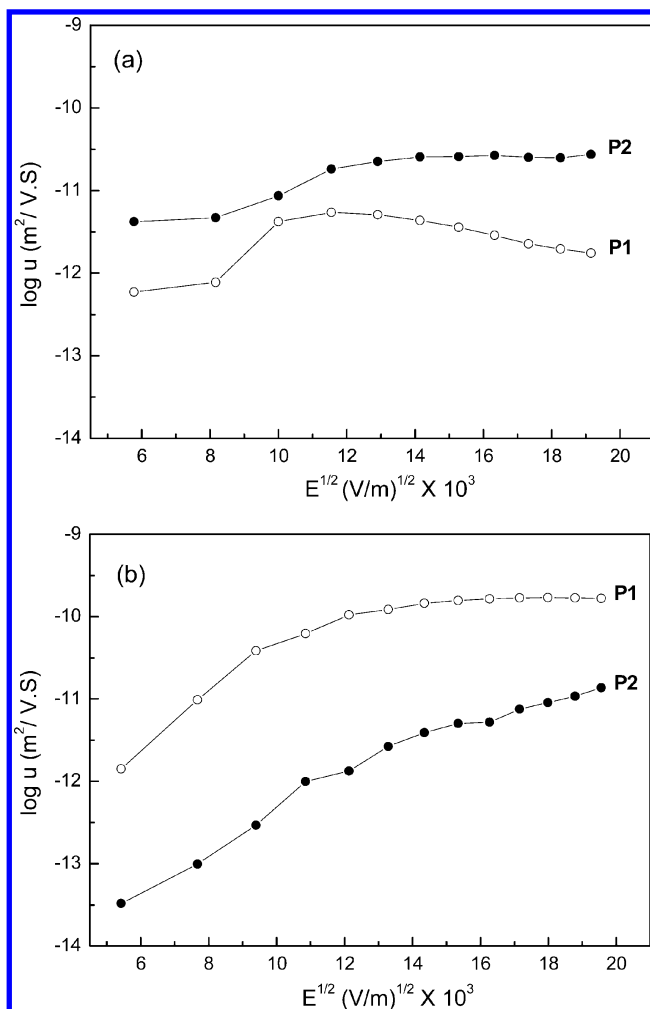

Figure 5. Brightness−voltage characteristics of polymers **P1**, **P2**, **P4**, **P6**, and **P7** in ITO/PEDOT/polymer/Ca/Al devices.

highly improved performance using copolymers as active layer, the hole-only and electron-only devices were made and characterized. Two polymers **P1** and **P2** were chosen to compare the hole and electron mobilities. The device structure of a typical hole-only device is ITO/PEDOT/polymer/Au. In this device hole injection is predominant, while electron is difficult to inject from cathode Au into polymer layer because of large energy barrier. Holes can thus be injected into polymer layer and pass throughout the device to measure its mobility. On the other hand, an electron-only device is fabricated with the configuration of ITO/Al/polymer/Ca/Al. In this case electron injection is relatively major and hole would be blocked between ITO and metal Al. Electrons can be injected into polymer layer and pass throughout the device to measure its mobility. The space charge limited current (SCLC) of single carrier is given by

$$J = 9\epsilon\epsilon_0 \mu V^2/8d^3$$

where $\epsilon\epsilon_0$ is the permittivity of polymer, μ is the carrier mobility, and d is the film thickness.[22] Figure 6a shows hole mobility (log μ) vs electric field ($E^{1/2}$) curve obtained from hole-only devices, and Figure 6b shows electron mobility vs electric field curve obtained from electron-only devices. For polymer **P1**, the electron mobility is approximately 2 orders in the magnitude higher than hole mobility, which indicates **P1** as an electron-transporting material. As reported in the literature, all

Figure 6. Mobility (log μ) vs electric field ($E^{1/2}$) curves in (a) hole-only and (b) electron-only devices.

PPV derivatives, except CN-PPV, have been found to be hole transport dominating. This is the first report that DP-PPV also owns electron-transport dominating property. The movement of hole and electron is obviously unbalanced and results in a poor device performance. For polymer **P2**, the hole and electron mobilities are nearly in the same order and charge balance is established. Combining the results form electrochemical and carrier mobility measurements, **P2** shows a promising potential for light-emitting application. Further investigation on interface injection and carrier mobility for other polymers will be continued.

Conclusion

Two series of poly(2,3-diphenyl-1,4-phenylenevinylene) derivatives containing long branched alkoxy or fluorenyl substituents were synthesized. Long and branched alkoxy chains were introduced to enhance the solubility for spin-coating process. Bulky diphenyl groups or fluorenyl substituents with two hexyl chains on the C-9 position were introduced to increase the steric hindrance and prevent the close packing of the main chain. DP-PPV derivatives with high molecular weights were obtained by controlling the feed ratio of different monomers during polymerization. All synthesized polymers possess high thermal stabilities which offer advantages under operation voltage. The maximum PL emission bands of thin films are located between 498 and 564 nm. Double-layer devices with the configuration of ITO/PEDOT/polymer/Ca/Al were fabricated and characterized. The devices emitted green to yellow-orange light under applied voltage. A maximum brightness of 16 910 cd/m^2 was observed for the devices fabricated with **P2** as the emissive layer. This is the highest value for DP-PPV derivatives reported in the literature so far. The results reveal that these materials are excellent candidates for PLED applications.

References and Notes

(1) Burroughes, J. H.; Bradley, D. D. C.; Brown, A. R.; Marks, R. N.; Mackay, K.; Friend, R. H.; Burn, P. L.; Holmes, A. B. *Nature (London)* **1990**, *347*, 539.
(2) Peng, Z.; Bao, Z.; Galvin, M. E. *Adv. Mater.* **1998**, *10*, 680.
(3) Bliznyuk, V.; Ruhstaller, B.; Brock, P. J.; Scherf, U.; Carter, S. A. *Adv. Mater.* **1999**, *11*, 1257.
(4) Politis, J. K.; Curtis, M. D. *Chem. Mater.* **2000**, *12*, 2798.
(5) Woodruff, M. *Synth. Met.* **1996**, *80*, 257.
(6) Braun, D.; Heeger, A. J. *Appl. Phys. Lett.* **1991**, *58*, 18, 1982.
(7) Greenham, N. C.; Moratti, S. C.; Bradley, D. D. C.; Friend, R. H.; Holmes, A. B. *Nature (London)* **1993**, *365*, 628.
(8) Chen, S. A.; Chang, E. C. *Macromolecules* **1998**, *31*, 4899.
(9) Wang, L. H.; Chen, Z. K.; Kang, E. T.; Meng, H.; Huang, W. *Synth. Met.* **1999**, *105*, 85.
(10) Chen, Z. K.; Huang, W.; Wang, L. H.; Kang, E. T.; Chen, B. J.; Lee, C. S.; Lee, S. T. *Macromolecules* **2000**, *33*, 9015.
(11) Wan, W. C.; Antoniadis, H.; Choong, V. E.; Razafitrimo, H.; Gao, Y.; Field, W. A.; Hsieh, B. R. *Macromolecules* **1997**, *30*, 6567.
(12) Hsieh, B. R.; Wan, W. C.; Yu, Y.; Gao, Y.; Goodwin, T. E.; Gonzalez, S. A.; Feld, W. A. *Macromolecules* **1998**, *31*, 631.
(13) Hsieh, B. R.; Yu, Y.; Forsythe, E. W.; Schaaf, G. M.; Feld, W. A. *J. Am. Chem. Soc.* **1998**, *120*, 231.
(14) Li, A. K.; Yang, S. S.; Jean, W. Y.; Hsu, C. S.; Hsieh, B. R. *Chem. Mater.* **2000**, *12*, 2741.
(15) Yang, S. H.; Chen, J. T.; Li, A. K.; Huang, C. H.; Chen, K. B.; Hsieh, B. R.; Hsu, C. S. *Thin Solid Films* **2005**, *477*, 73.
(16) Li, Y. C.; Chen, K. B.; Chen, H. L.; Hsu, C. S.; Tsao, C. S.; OuYang, W. C.; Ho, D. L.; Chen, S. A. *Macromolecules*, in press.
(17) Antoun, S.; Karasz, F. E.; Lenz, R. W. *J. Polym. Sci., Part A: Polym. Chem.* **1988**, *26*, 1809.
(18) Neef, C. J.; Ferraris, J. P. *Macromolecules* **2000**, *33*, 2311.
(19) Chen, C. H.; Tang, C. W. *Appl. Phys. Lett.* **2001**, *79*, 3711.
(20) Liao, J. H.; Benz, M.; LeGoff, E.; Kanatzidis, M. G. *Adv. Mater.* **1994**, *6*, 135.
(21) Henckens, A.; Colladet, K.; Fourier, S.; Cleij, T. J.; Lutsen, L.; Gelan, J.; Vanderzaande, D. *Macromolecules* **2005**, *38*, 19.
(22) Xia, Y.; Friend, R. H. *Macromolecules* **2005**, *38*, 6466.